

# Mask repair using layout-based pattern copy for the 65-nm node and beyond

Volker Boegli<sup>\*a</sup>, Nicole Auth<sup>a</sup>, Uli Hofmann<sup>b</sup>

<sup>a</sup>NaWoTec GmbH - A Carl Zeiss SMT Company, Industriestr. 1, D-64380 Rossdorf, Germany

<sup>b</sup>GenISys GmbH, Forststr. 39a, D-85521 Riemerling, Germany

## ABSTRACT

To overcome several drawbacks of the standard pattern copy procedure used to create the repair shape(s) for a particular defect site, we have developed and implemented a layout based pattern copy method (a.k.a. “database pattern copy”). In general, pattern copy derives the repair structure by comparing a high resolution image of the defective area with the same image of a non-defective area. The repair shape is generated as the difference of these two images, and adjusted for processing purposes. As opposed to the conventional pattern copy method, which derives the reference using information taken from the mask under repair, the new method uses reference information from the *original mask design file*. As a result, it reduces the CD error of the repair, simplifies the repair process work flow, and greatly reduces the potential of operator error. We present the new method along with experimental results taken from programmed defect repair on our MeRiT MG™ production tool.

**Keywords:** Mask repair, pattern copy, process control, layout, database

## 1. INTRODUCTION

Recent advances in mask repair technology have slowed the projected cost explosion in mask production. As we progress towards the 45 nm node, electron-beam induced deposition and etching has proven to be the most likely candidate capable of meeting the stringent repair specifications. Utilizing the e-beam platform’s fast, high-resolution imaging capability, the repair work flow contains a method frequently called “pattern copy”, which derives the repair structure by comparing a high-resolution image of the defective area with the same image of a non-defective area. The repair shape is generated as the difference of these two images, and adjusted for processing purposes. Due to the excellent imaging capability of our Gemini column, combined with sub-pixel resolution of the image processing algorithm, shapes are generated and placed with an accuracy of a few nanometers. This method has proven to ultimately reduce post-repair CD errors since manual drawing of the repair outline is no longer necessary, and has become the method of choice for our repair tool.

Conventionally, the pattern copy reference image is taken from the mask under repair. For this method to work, a suitable area containing a non-defective feature, identical to the defective feature, has to be identified on the mask and imaged. In general, this works well, however there are several drawbacks. For one, all the inaccuracies of the reference feature, like line edge roughness (LER), CD error, and imaging artifacts will be transferred to the repaired spot. Secondly, a slight variation from the target size of the scan field goes unnoticed and leads to additional CD error after repair. Furthermore, logic designs may make it hard to find identical reference areas, especially for larger defects. And finally, a feature similar in shape and size to the defective feature may be mistakenly used, again leading to CD error.

To overcome these drawbacks, we have developed layout based pattern copy (“database pattern copy”). In this case, the reference is generated using information taken from the original mask design file. This is the file which was used to write the mask in the first place, and it contains the exact reference information we need to perform a pattern copy step. We create an image of the features inside the applicable field of view, and render this image according to a specified set of criteria, with the aim to make it look exactly like the image taken from the mask. The rendering step is necessary to emulate and compensate the basic characteristics of mask writer, manufacturing process, and image formation in our e-beam tool.

---

\* boegli@smt.zeiss.com

The pattern copy process then continues as usual, only with the “ideal” reference image instead of the “real” reference image from the mask. As a result, we achieve a reduction in the CD error of repaired features, with the side benefit of greatly improved work flow, since the reference is automatically generated and aligned to the defect.

In this paper we compare mask repair using conventional pattern copy (reference taken from the mask) to layout based pattern copy, and demonstrate the overall improvement in repair quality. This is manifested in reduced CD variation of repaired features, and verified by CD-SEM and AIMS™ measurements. We also highlight the improvements in work flow, and show the potential of further automation in the repair process.

## 2. PATTERN COPY WORK FLOW

### 2.1 Standard pattern copy

A standard defect repair involves navigating to the defect site, usually according to position information of the inspection file, and centering the defect to fit into the repair field of view. A high resolution image is obtained using selectable scanning parameters which have been optimized for a particular mask type. After review of the defect shape, a suitable reference has to be found which covers at least the defect area and which is defect free. In the best case, this reference is located within the already scanned image, so the user can simply identify the region without having to navigate around. In the worst case, the reference is far away from the defect site and thus involves a search on the mask and navigating back to the defect. Once the reference has been identified, the image is scanned again and drift correction areas are identified to support the active drift correction. To initiate repair shape generation, the reference is roughly placed over the defect. The system precisely aligns the two images and derives the repair shape (or several shapes, depending on the complexity of the defect).

A sequence of images obtained during a standard pattern copy procedure is depicted in Fig 1. The first picture is the original defect image of a programmed protrusion. Physical pixel size is 2 nm and the secondary electron signal is used for image formation. Characteristic of the SE signal is a strong topographic contrast which enhances the feature edges. The second picture shows the reference image obtained from another location on the mask, and taken using the same scanning parameters as for the defect image. The frame inside the image has been added by the operator and identifies the portion of the image which is to be used as the reference area. In the third picture, the reference is seen to have been roughly placed over the defect. Finally, the last picture shows the created repair shape after automatic alignment of reference and defect.

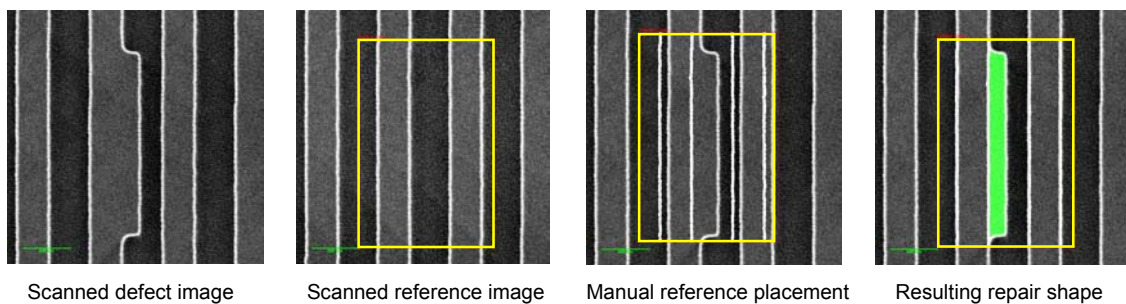


Fig. 1: Example of a standard pattern copy sequence (MoSi protrusion programmed defect)

## 2.2 Database pattern copy

When the original layout is available and has been loaded from a database, the procedure is a lot simpler. After the defect image has been obtained and drift correction areas have been identified, the repair shape is created with the simple push of a button. The system automatically performs all necessary steps to create a suitable reference image from the original layout. This includes creation and rendering of the layout image, pre-alignment to the defect image, and precise mapping of the resulting reference image to the defect image to correct for shift, scaling, and rotation/orthogonality errors. Standard and database pattern copy work flows are compared side by side in Fig. 2.

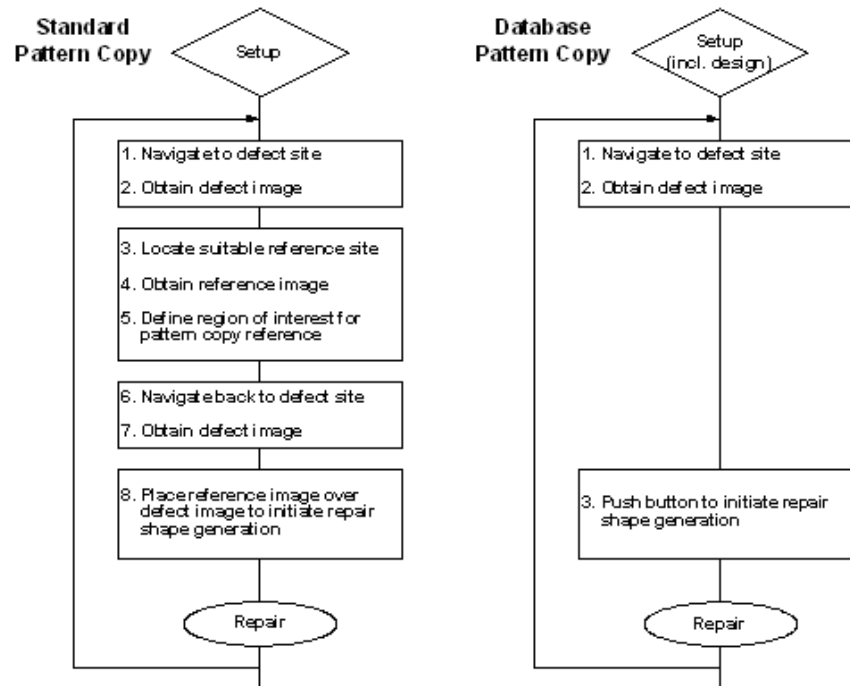


Fig. 2: Work flow comparison: standard versus database pattern copy

## 3. AUTOMATION

### 3.1 Design data reader

Access to the mask design layout data is provided by a third-party commercial software package (Layout ENGINE of GenISys GmbH). This package has been designed in close collaboration between GenISys and Zeiss, and meets our requirements for use in a mask shop environment. It transparently supports a variety of mask writer data formats, while a standardized interface is presented to the application that includes the package. This allows to support additional file formats in the future without impacting the main application software.

Layout Engine is a robust, flexible and modular high-performance layout database & toolset for integration into custom applications. The Layout ENGINE native database format LEDB with geometrical sorting enables extremely fast access and extraction (regions, layer, cells). The size of layout is not limited by the system memory. Large layouts (> 20 GB) in GDSII or e-beam machine formats can be imported with approx. 1GB/min, close to the disk I/O rate (see Fig. 3).

A large variety of different generic layout data formats (GDSII, DXF, CIF, TXL) and e-beam data formats (MEBES, NuFlare/Toshiba VSB 11 / 12, JEOL 52 V 3.0) are supported. Additional formats will be implemented upon request.

The native high performance database format LEDB provides a standardized interface regardless of underlying layout data format and enables fast extraction of regions of interest (ROI) and shapes within seconds. Layout ENGINE also offers optional layout transformation (size, rotate) and processing functions (bias, heal, tone reversal, Boolean operation, etc). The Layout ENGINE module is tightly integrated into the MeRiT repair software using a lean and efficient C++-API interface.

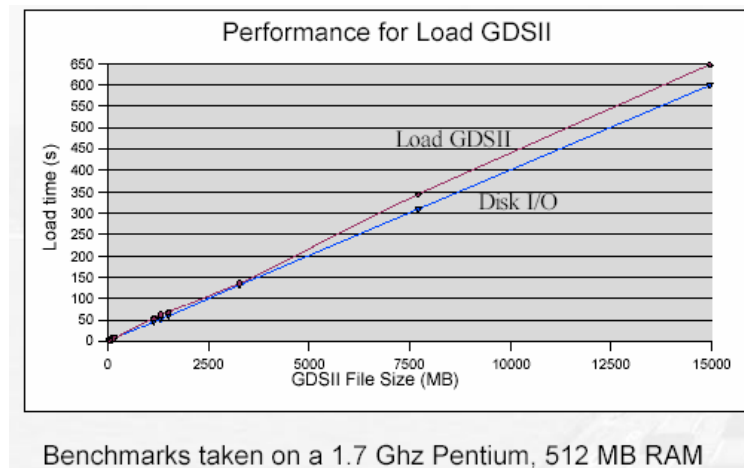


Fig. 3: Import of large layout data close to disk I/O rates (only 10% overhead)

### 3.2 Reference image generation

An automated sequence is used to create the reference shape when an appropriate layout file has been loaded upon repair job setup. First, information about the current field of view is sent to the design reader module. This information includes current location on the mask, as well as the physical size of the current field of view. In return, the design reader submits a list of all shapes which are fully or partially contained inside this field of view. Next, the shapes are scaled and drawn on a virtual image canvas with equal properties to the images obtained from the defect. The result is an image of the original layout which roughly corresponds to the features seen on the mask. This image is now rendered according to a set of selectable parameters, with the aim to make the defect-free portions look as similar to the scanned defect image as possible. Finally, the rendered image is precisely aligned to the defect image, and the repair shape is created as the difference of the two images. Fig 4 summarizes the automated flow of reference image creation.

An example of the sequence described above is given in Fig 5. The first picture (1) shows the scanned defect image from the mask. In the second picture (2), the relevant shapes have been extracted from the database and drawn. Note that these shapes bear geometric information only (rectangles and polygons), and can therefore only be drawn as blocks in either normal or reverse tone. In our case, the shapes are bright on a dark background. The third picture (3) shows how the image changes after rendering, and that it now looks like an “idealized” version of the image obtained from the mask. This rendering step is the most important step, since the accuracy of the resulting repair highly depends on it. The rendering parameters are chosen to emulate basic characteristics of the mask writer, resist development and etch processes, and image formation in the MeRiT tool. The rendered image has also been precisely aligned to the defect image, taking into account any residual offset, scaling, rotational, and/or orthogonality errors of the defect image which was obtained from the mask. In a final step, the shape or shapes to be scanned by the e-beam during the actual repair process is generated, and the result is shown in picture (4) of Fig 5. The shape edges are smooth and do no longer exhibit the imperfections (roughness, jogs etc) of the features on the mask. From here, the repair continues the same way as if the shape had been created by conventional pattern copy.

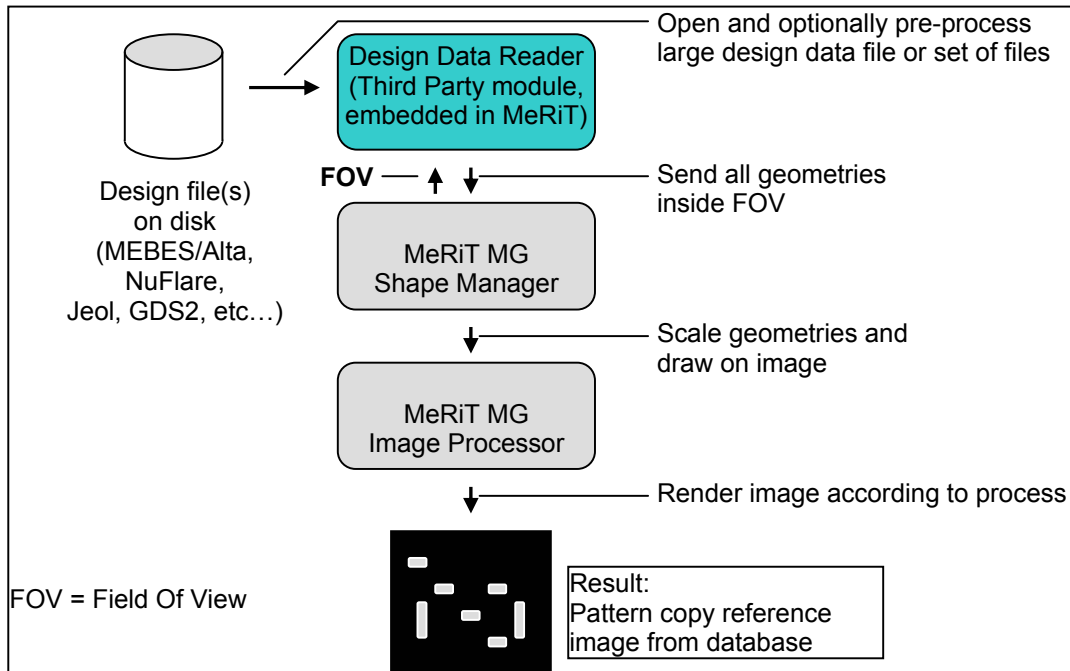


Fig. 4: Design reader processing flow: layout shape extraction, conversion to image, and rendering

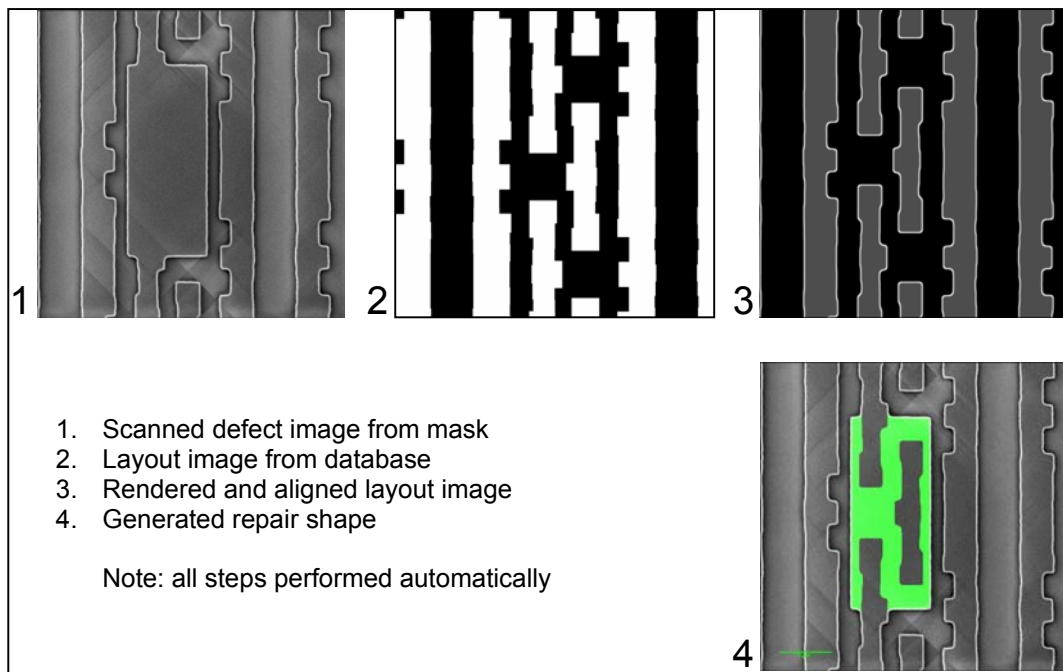


Fig. 5: Example of fully automated database pattern copy sequence

## 4. COMPARISON USING PROGRAMMED DEFECTS

### 4.1 Experiment

To verify the assumption of a reduced repair CD variation, two sets of repairs were carried out, one using conventional pattern copy, and the other using database pattern copy. The defects used are programmed protrusions on a MoSi lines and spaces pattern, which facilitates the AIMS evaluation. A sample repair for both methods is shown in Fig 6; each sequence shows the defect image, the reference image, and the resulting repair which is highlighted in the post-repair image. Note the differences in the reference image, and the slightly smoother edge after repair for database pattern copy. Independent FC-SEM measurements of the features confirmed the expected reduction in line edge roughness of the database pattern copy repair, which is simply due to the fact that the reference edge was perfectly straight.

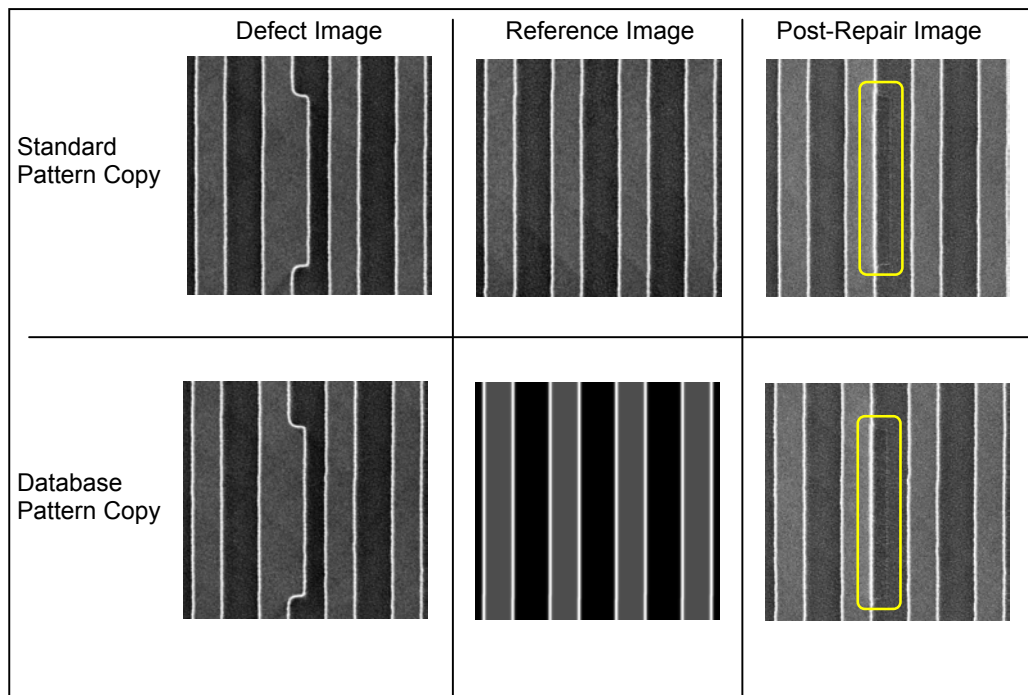


Fig.6: Repair of programmed MoSi protrusions, using standard and database pattern copy

Five repairs of each kind were performed, using the conventional pattern copy and the database pattern copy methods, respectively. Care was taken that a new reference was used for each repair, to emulate real-world conditions on production defects, although for this experiment the defects were identical. After repair, AIMS CD measurements were taken for each repair site, using a standard procedure which also takes into account effects of the repair site on adjacent features. A sample AIMS evaluation is given in Fig. 7. A threshold defining the line width is determined such that the reference is scaled to nominal size, and used for all measurements. Intensity profiles of the defect site and a reference site are plotted, along with a line width versus defocus series.

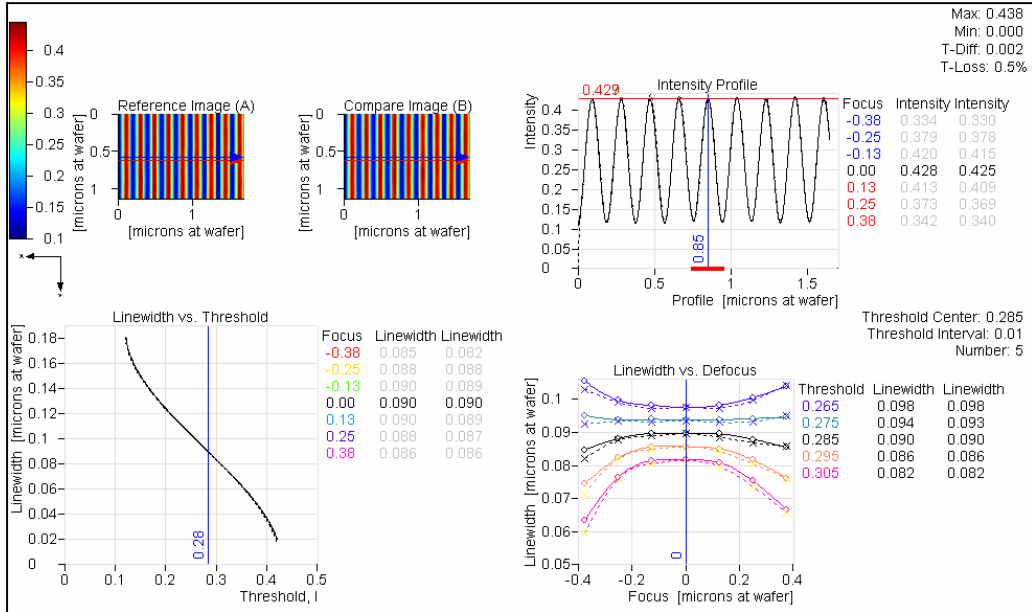


Fig. 7: Example of AIMS™ CD evaluation

## 4.2 Results and discussion

The results of AIMS CD measurements are presented in Fig. 8. The upper table represents repairs using the new database pattern copy method, while the lower table covers the standard repairs. For each repair site, the “space” dimension at the repair site is taken, plus measured dimensions of the left and right adjacent line (blue columns in Fig. 8). The same measurements are taken from the reference site which did not contain a defect (black columns in Fig. 8). “LA” stands for “left adjacent”, “RA” for “right adjacent”. At the bottom of each column, the CD mean and 3-sigma values are listed. Note that the sigma is given in nanometers, while the common definition of AIMS CD is in % of nominal line width. The target width of the space is 90 nm, while the target width of the adjacent lines is 100 nm.

Although there appears to be a systematic deviation of repaired to target CDs, the 3-sigma values are within the target specification of 5%. The systematic deviation is attributed to two independent effects: a) there was a stronger than usual drift in the tool at the beginning of the database repair series, and b) the rendering parameters had been chosen in a first approach by visually comparing the rendered reference image with the defect image. The column labeled “Repair Space” contains measurements at the repair site. For our purpose of comparing the two pattern copy methods, the 3-sigma value is the relevant figure. Database pattern copy yields a 3-sigma of 3.1 nm, while the conventional method results in a 3-sigma of 4.8 nm. Incidentally, this value is the only one marginally above spec (= 5% of 90 nm = 4.5 nm). This proves our assumption of reduced CD variation when an “idealized” reference is used. We expect the difference to become even larger after an automated routine has been developed to optimize the parameters of the shape rendering step, which is currently ongoing.

### Critical dimensions of repaired space and adjacent lines (AIMS™ CD)

	LA Ref Line	LA Repair Line	Ref Space	Repair Space	RA Ref Line	RA Repair Line	
Reference from layout	Repair 1	99	99	90	87	99	102
	Repair 2	99	101	91	87	98	102
	Repair 3	99	100	90	86	99	103
	Repair 4	99	101	88	89	99	100
	Repair 5	101	100	87	88	101	100
	Mean	99.4	100.2	89.2	87.4	99.2	101.4
	3 sigma (nm)	2.40	2.24	4.41	3.06	2.94	3.60
Reference from mask:	Repair 1	99	100	90	88	100	101
	Repair 2	99	100	87	86	101	102
	Repair 3	99	99	89	90	99	99
	Repair 4	99	99	89	90	99	100
	Repair 5	98	98	90	90	99	100
	Mean	98.8	99.2	89	88.8	99.6	100.4
	3 sigma (nm)	1.20	2.24	3.29	4.80	2.40	3.06

Fig. 8: AIMS™ CD results for 5 programmed defect repairs each, database and standard pattern copy

## 5. CONCLUSION

In summary, our recently implemented layout based pattern copy procedure has met the expectations of simplified work flow, reduced CD error of the repair, and generally reduced potential of operator error. It eliminates a series of manual steps necessary during standard pattern copy, thus increasing repair throughput and productivity. The experimental side-by-side comparison of the two methods resulted in a reduced CD error of 3.1 nm (3-sigma) for database pattern copy, versus 4.8 nm (3-sigma) for standard pattern copy. These were the first experimental results, and further improvement is expected after a refined procedure for rendering parameter determination has been implemented. Layout based pattern copy could play a crucial role for future technology nodes (45 nm and below) since the corresponding CD error specifications become progressively tighter. The new feature is fully integrated in the MeRiT MG repair application and ready to be used in a production environment.

## REFERENCES

1. K. Edinger, V. Boegli, W. Degel: Performance results from the Zeiss/NaWoTec MeRiT MG electron beam mask repair tool, Photomask and Next-Generation Lithography Mask Technology XII, Proc. SPIE Vol. 5853, paper 5853-129, pp 361-370, 2005
2. A.R. Stivers, P.Y. Yan, G. Zhang, T. Liang, E.Y. Shu, E. Tejnil, B. Lieberman, R. Nagpal, K. Hsia, M. Penn, and F. C. Lo: EUV Mask Pilot Line at Intel Corporation, 24th Annual BACUS Symposium on Photomask Technology, Proc. SPIE Vol. 5567, paper 5567-03, 2004
3. T. Liang, E. Freundberg, D. Bald, M. Penn, and A.R. Stivers: E-beam Mask Repair: Fundamental Capability and Applications, 24th Annual BACUS Symposium on Photomask Technology, Proc. SPIE Vol. 5567, paper 5567-49, 2004
4. W.H. Press, B.P. Flannery, S.A. Teukolsky, W.T. Vetterling: Numerical Recipes in C++, Cambridge University Press, 2002, ISBN 0-521-75033-4